Investigation of the Minimum Detectable Activity Level of a Preclinical LSO PET Scanner

Nicolas Karakatsanis, *Student Member, IEEE,* Qinan Bao, *Student Member, IEEE,* Nam Vu, *Student Member, IEEE* and Arion Chatziioannou, *Member, IEEE*

***Abstract*–Novel molecular imaging applications increasingly involve studies where very low amount of activity is present. This operation point can be challenging in terms of image quality especially when the intrinsic detector activity from scintillators such as LSO is considered. LSO crystals contain ^{176}Lu which emits β^- particles followed by γ photons, resulting in the detection of true and random events. This background activity has been shown to contribute a significant percentage of the total detected true events, when a very weak activity distribution is imaged. This can affect the weakest signal that can be detected by an LSO PET scanner which determines its "detection limit" and is evaluated by the parameter of minimum detectable activity or MDA. A series of acquisitions was performed in order to study the effect of the energy window to the intrinsic true and randoms rate. The experiments were also simulated with GATE, and the results were validated by comparing them with the experiment. Four square regions each with a unique signal to background activity concentration ratio were used. The background activity level was held constant between the different regions, while the activity of the point sources varied in 4 selected levels. The signal to background ratio was calculated separately for each region. The energy spectrum of the intrinsic background activity and its contribution to the total energy spectrum both for singles and coincidences was estimated through the GATE simulation. We histogrammed both the measured and simulated data on various time frames, which we reconstructed using the Filtered Backprojection algorithm. Every image was quantified based on the Currie equation in order to associate an MDA value for each of the 4 point sources as a function of the frame length. In the case of the microPET Focus 220 a total amount of 4nCi/mm^3 can be reliably detected for frame lengths longer than 5min and at regions where the signal to background activity concentration ratio is higher than 4. In the case of higher contrast regions detection can be achieved even for frame lengths down to 1min.**

I. Introduction

One of the most important parameters that characterize the performance of a PET scanner is sensitivity. Small animal PET systems have been designed in such a way that can acquire sufficient number of counts, when they operate at relatively low activity levels that are usually present in small animal imaging studies.

Manuscript received November 16, 2007.

N .Karakatsanis is with the Department of Electrical and Computer Engineer, Biomedical Simulations and Imaging Laboratory of the National Technical University of Athens, 9 Iroon Polutechniou St., 15780, Athens, GR

Q. Bao, N. Vu and A.F.Chatziioannou are with the Crump Institute for Molecular Imaging, University of California, Los Angeles, 90095, Los Angeles, CA, USA.

This work was supported in part by UCLA SAIRP NIH-NCI 2U24 CA092865.

However, novel molecular imaging applications have brought the need to image very weak sources of less than 10nCi activity. Therefore an additional performance parameter was used to evaluate the ability of a PET scanner to detect and image very low levels of activity distributions: the minimum detectable amount of activity or MDA.

In this study we will define the MDA parameter as the minimum mean number of net counts that are necessary to produce an image where the probability of having false positive or false negative detection is reduced to 5%. The Currie equation (1) provides an estimate of the MDA which is proportional to the standard deviation of the background activity at a specific Volume of Interest (VOI) [1]

$$MDA = 4.653\sigma_{bkgrd} + 2.706 \qquad (1)$$

The importance of this parameter increases when it is referring to ^{176}Lu-based PET scanners because of the non-negligible background count rate they create, due to the intrinsic radioactivity of ^{176}Lu. The decay scheme of ^{176}Lu produces β^- particles (420keV) in cascade with γ photons of energies of 307keV (94%), 202keV (78%) and 88keV (15%) [2]. We have measured that the total intrinsic activity of the microPET Focus 220 in the entire FOV volume to be approximately 4μCi. When a source with activity on the order of tens of nCi is imaged, then the standard deviation of background originating from the scintillator crystals can significantly raise the detection limit set by Eq.(1). Consequently the ability to detect point sources within a uniform background activity region is also adversely affected. [3-5]

In this study we are interested in evaluating the counting performance of the small animal LSO-based microPET Focus 220 scanner, using the MDA parameter, when point-like activity concentrations of less than 5nCi/mm^3 are placed within a uniform background activity region for different acquisition lengths.

II. Materials and Methods

Our initial purpose was to study the effect of the energy window to the intrinsic trues and randoms rate of the microPET Focus 220 system, because the calculation of the MDA parameter is strongly related to these background count rates. Recent imaging studies have shown great dependence between the intrinsic true and random rates and the choice of the energy window applied when very low amounts of activity

are imaged. [2] For this reason a series of blank scans was performed without a source in the FOV of the scanner. We started from a large energy window of 255-766keV, around the 511keV photopeak. The window width was then reduced to 40%, 30%, 20% and 10%.

Subsequently the same series of experiments was simulated with GATE, a well validated and supported Monte Carlo simulation package specially designed for nuclear medicine applications [6]. The LSO intrinsic activity was simulated by using an ion source of ^{176}Lu confined to the detector volume of the system. Our purpose was to validate the simulation results by comparing them with the respective experimental data.

We also used a modified inkjet printer in order to print F-18 activity distributions on four glossy papers which were placed perpendicular to the scanner bed, in a transaxial orientation, along the axis of the detector rings. The use of inkjet printing technology allowed us to accurately design and print uniform activity distributions as well as point sources of 1mm^2 surface. On each paper a 15x15mm^2 constant background activity distribution was printed together with a 1mm^2 point source of varying activity level representing the signal.

We selected point-like activity distribution for our signal because we are particularly interested in evaluating the ability of the imaging system to accurately count this sample and discriminate it from the rest of the background activity. The point source size was chosen to be less than the reported spatial resolution for this system of 1.75mm [7]. The four printed sources were surrounded by a water-equivalent material provided by Computerized Imaging Reference Systems (CIRS Inc., Norfolk, VA) to ensure annihilation of emitted positrons. The geometric configuration we used is shown at figure 1. This set-up allowed us to acquire data from all four different contrast regions simultaneously.

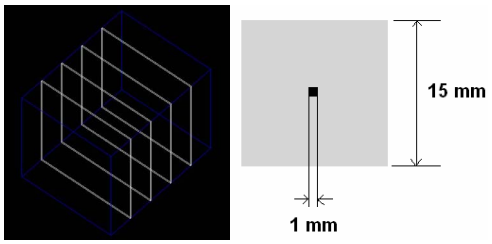

Figure 1. Geometric configuration of the four plane activity distributions in a transaxial orientation along the axis of the scanner (left) and relative position and dimensions of the printed point source and the background source (right)

The measured activity concentration for the four point sources starting from the highest-contrast region is approximately 4, 3, 2 and 1nCi/mm^3, whereas the background activity concentration was measured to be approximately 330pCi/mm^3 for all contrast regions. The signal to background activity concentration ratio (SBR) for each of the four regions was calculated by taking the ratio of the sum of the measured point source and background activity distribution to the measured background activity distribution and is presented at Table I.

TABLE 1
SIGNAL TO BACKGROUND ACTIVITY CONCENTRATION RATIOS

Region Type	A	B	C	D
Signal to Background Ratio (SBR)	6.7	5.3	4.5	2.9

We performed a 10min acquisition, using the large energy window of 250-700keV, which is the standard window of microPET applied for most small animal imaging studies. This window is selected to maximize the scanner sensitivity [8]. The data was histogrammed in time frames of 30sec, 1min, 2min, 5min and 10min. These acquisition times are realistic and compatible with routine operation of a small animal imaging resource [8].

A 3D FBP reconstruction algorithm was used and the images were analyzed to estimate the MDA value for each region as a function of the frame length.

In this particular study the source signal is low enough to ensure that it does not affect the calculation of the MDA value. Its contribution to the minimum detectable activity is negligible and, therefore it is safe to ignore the constant term of Currie equation (1) and transform it to the following simplified equation

$$MDA = 4.653\sigma_{\text{bkgrd}} \qquad (2)$$

resulting in a lower MDA threshold [1].

In order to quantify the image data we drew an ROI at each of the four point sources and a relatively larger ROI at the background of each region. The maximum signal pixel value and background standard deviation were measured.

The mean pixel value of the background ROI was subtracted from the maximum pixel value of the respective signal ROI to estimate the maximum net signal counts. The measured background standard deviation was used to calculate the MDA value according to Eq. (2). Finally the ratio of the maximum net signal counts to the MDA value was calculated to decide whether the measured number of counts in a signal ROI came from the actual point source or the background. If the ratio is higher than unity, then we can claim with an uncertainty of 5% that in this case a real signal was detected by the PET imaging system and activity was present within this ROI.

Furthermore, the above experiment was simulated with GATE to determine the energy spectrum of the intrinsic LSO background singles and coincidences. The respective contribution of the scintillator background to the total energy spectrum when the four background and four signal sources

are present in the FOV was also determined. The geometry set-up of this GATE simulation is depicted at figure 2.

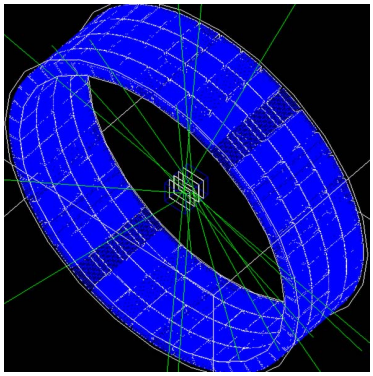

Figure 2. GATE simulation geometry configuration. The four activity distributions were placed in a transaxial orientation along the axis of the scanner. Sample trajectories of the annihilation photons can be seen

Identical activity and attenuation concentrations with the experimental data were simulated and the output data were histogrammed into the same time frames. We used STIR's FBP-3D reprojection to reconstruct the projection data and obtain the images [9]. The same ramp filter settings were selected both for experimental and simulated data.

The MDA quantification analysis for the simulated image data was repeated and the results were compared with the experimental data.

III. RESULTS AND DISCUSSION

A. Energy window effect on intrinsic background count rate

The experimental and simulated count rate for both trues and randoms (delays) in the case of the microPET Focus 220 system for five different energy windows is shown on figures 3a and 3b respectively. The experimental data were acquired for 14 hours whereas in the case of simulation a 5sec acquisition length was used to keep the CPU time of the simulation to an accepted level. Both count rates were scaled to a single acquisition length of 1sec. Since a single number was derived from the simulation, statistical noise was not an issue in the short duration of the simulated acquisition.

The location of the 511keV photopeak was used as a reference for all the different energy windows. Starting from a large window with a 50% size, we gradually reduced the width to 40%, 30%, 20% and 10%.

The intrinsic trues rate decreased by half when the energy window was limited from 50% to 40% and became negligible at 30%, i.e. when the low level energy discriminator is approximately at 358keV. At the same time the intrinsic randoms rate was also reduced and always remained at low levels compared to the intrinsic trues rate. Therefore we conclude that when a 255-766keV window is applied (50% of the reference length), which is often used in small animal imaging studies, the intrinsic count rate becomes significant for studies involving very low amounts of activity concentrations, i.e. in the order of a few nCi/mm^3. A possible solution would be the reduction of the window length at 30% of the 511keV reference value. However this will result a significant decrease of the sensitivity of the microPET system. In the following studies we have chosen to operate our system at the standard large energy window of 250-700keV, because we would like to investigate how the LSO intrinsic count rate can affect the MDA value and consequently the detection limit of microPET when it operates with a standard window, i.e. when the contribution of the background count rate to the net signal count rate cannot be neglected.

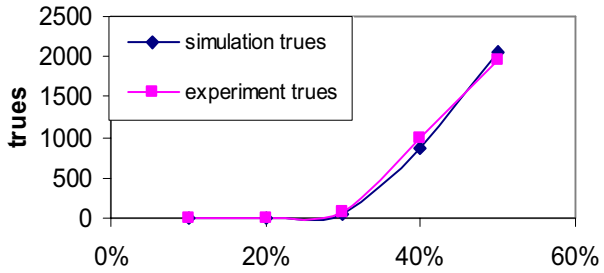

Figure 3a. Trues count rate vs. energy window length for simulated (blue) and experimental (red) data. The rates are scaled for 1sec acquisition length

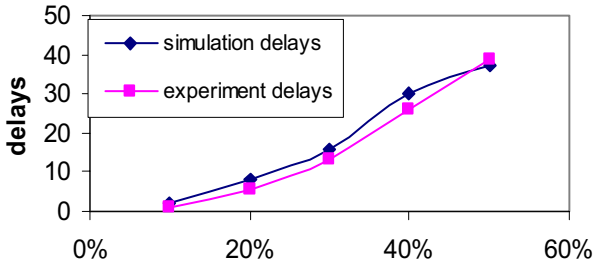

Figure 3b. Randoms count rate vs. energy window length for simulated (blue) and experimental (red) data. The rates are scaled for 1sec acquisition length

Figures 3a and 3b show a good agreement between the experimental and simulation datasets (less than 10% discrepancies) indicating that GATE has the ability to simulate the energy window effect on the low intrinsic count rates of LSO-based PET scanners accurately.

B. Characteristics of LSO background intrinsic activity

The coincidence energy spectrum of the LSO intrinsic background activity as well as the total coincidence energy spectrum of a simulated 1min acquisition of the four activity distributions in the microPET Focus 220 are presented at Fig. 4.

The ^{176}Lu energy spectrum contribution to the total coincidences energy spectrum is significant. We are observing an energy peak of the spectrum at 307keV, which is

caused by the gamma photons, and a wide distribution of the beta particles along the whole energy window. The analysis of the simulated data has shown that the numbers of beta and gamma particles that resulted in coincidences were very similar, leading us to the conclusion that almost all the coincidences were caused by the simultaneous detection of beta-gamma particle pairs. This result is expected, because the energy window used for the simulated acquisition was between 250-700keV and therefore only one peak of the gamma emission spectrum could have been detectable, reducing the probability for a gamma-gamma coincidence event dramatically.

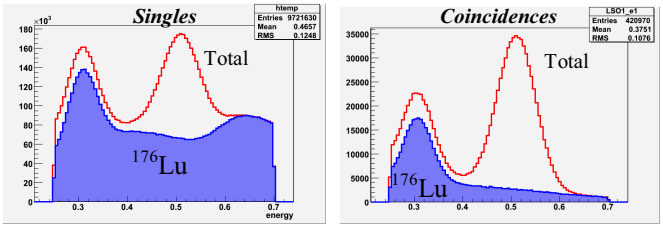

Fig. 4. Singles (left) and coincidences (right) energy spectrum. Total coincidences energy spectrum (red line) and coincidences energy spectrum of the ^{176}Lu intrinsic activity (curve filled with blue color). An energy window of 250-700keV has been used.

C. Performance analysis of microPET Focus 220 based on Minimum Detectable Activity parameter

The reconstructed images for 10min, 5min and 1min acquisition frames obtained from the experimental data are presented in Fig. 5. Each frame consists of four different contrast regions. The measured signal to background ratio for each is given at Table I.

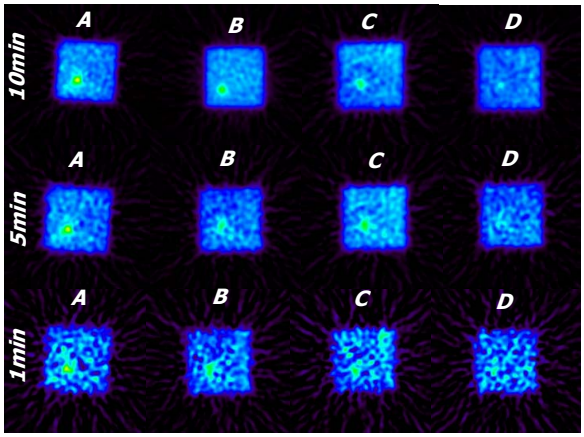

Fig. 5. Image data reconstructed for 10min, 5min and 1min experimental acquisition frames. Each frame consists of 4 different signal to background ratio regions, beginning at left with the highest ratio (region A) and ending to the right with the lowest ratio region (region D)

The equivalent images obtained from simulated projection data are shown at Fig. 6.

Visual observation of the experimental image data indicates that a point source over a background activity distribution can be detected from the microPET LSO scanner when data is acquired for at least 10min and the signal to background ratio (SBR) is higher or equal to 2.9, (region D). Moreover if the SBR of the imaging distribution is higher (region C) the acquisition length can be reduced down to 5min. Finally if the SBR is 6.7, equivalent to region A, or higher, then 1min acquisitions should be adequate for detection of the point source from the background activity.

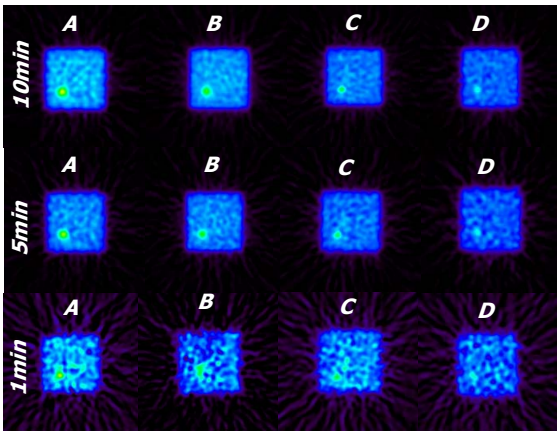

Fig. 6. Equivalent image data from 10min, 5min and 1min simulated acquisition frames.

The simulated data follow a similar trend. Point sources for all contrast regions were detected in the case of the 10min and 5min acquisition frames. However when a 1min simulation was performed only the point source at region A could be resolved.

The main reason for the differences between the experimental and the simulated images is believed to be the fact that the normalization and attenuation corrections were not applied to the simulated data. However these discrepancies between the two datasets do not appear to affect the results except from the case of region D of the 5min frame. In that case, the experimental data are more likely to result in a false-negative decision about the detection of a point source than the simulated data.

Because of the uncertainty introduced by visualization, we use the MDA parameter as defined by Eq. (2) to quantify the ability of this LSO-based small animal scanner to reliably detect point-like activity distributions surrounded by a uniform background region, for different signal to background ratios and acquisition times.

After the ROI quantification analysis, Fig. 7 shows the data points that represent the ratio of the maximum net counts detected at a pixel of a signal region, to the MDA value for all the four regions and for acquisition frames of 10min, 5min, 2min, 1min and 30sec. If the ratio is higher than one the detectability condition set by the Currie equation is satisfied and our point source distribution is considered to be detected with a 5% error probability.

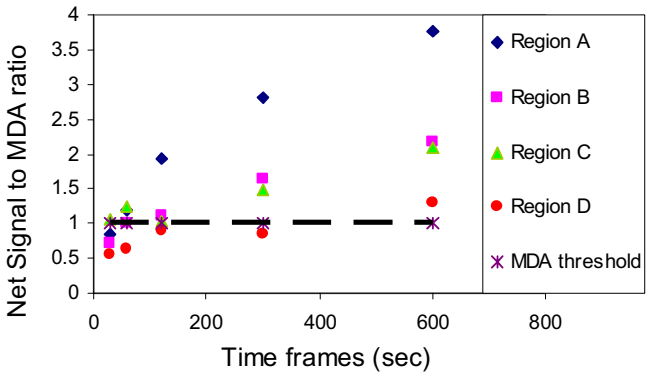

Fig. 7. Net signal counts to MDA value ratio for the experimental data as a function of different time frame durations and for different signal to background regions.

This quantification analysis was repeated for our simulated data as well and the results are shown at Fig. 8.

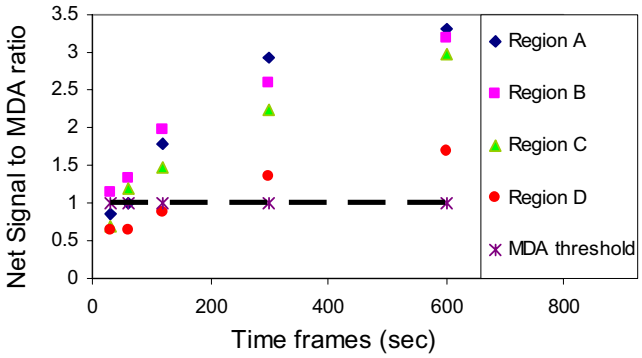

Fig. 8. Net signal counts to MDA value ratio for the simulated data as a function of different time frame durations and for different signal to background regions.

From the experimental results we conclude that the microPET Focus 220 scanner has the ability to reliably count very weak point sources of approximately 4nCi/mm^3 concentration inside a uniform background, if the frame length is 5min or longer and the SBR is equal or higher than 4.5. This is the value corresponding to region C. However, if our SBR value is improved up to 5.3 or higher, equivalent to region A and B, then a total frame length of 1min is adequate to ensure detectability.

In the case of the simulated data, we reached the same conclusions except when a SBR value of 2.9 is used with a total frame length of 5min. Generally we obtain better contrast ratios for simulated data and we believe that the main reason for this, in addition to the reasons described at the previous section, is possible differences in the way ROIs were drawn on experiment and simulated data as well as the different FBP implementations used for the reconstruction of the two datasets. Nevertheless these differences do not appear to affect the outcome of the MDA quantification analysis regarding the acceptance of a count as a reliable detection or as a false-positive measurement that has to be rejected. Moreover the trade-off between the SBR value of our imaging sample and the length of the acquisition frame is also obvious from these results.

This study has been conducted at a pre-clinical LSO-based small animal scanner which is used extensively nowadays for research purposes. However, applications involving very low amounts of activity are important in human clinical imaging studies where the imaging systems have very different geometric characteristics that can significantly affect the calculated MDA value. Therefore we are planning to expand this analysis for LSO clinical systems as well and investigate its behavior when different energy windows are applied.

IV. CONCLUSIONS

In this study it was shown that very weak sources with activity concentration of 4nCi/mm^3 can be reliably detected by the microPET Focus 220 system when the standard energy window of 250-700keV is applied. That is, provided that the signal to background ratio of the targeted regions and the acquisition frame length meet the MDA requirements.

A trade-off between the SBR and the acquisition frame length was also identified as expected. In general, longer acquisition times should lead to lower detection thresholds.

The simulation study with GATE reproduces the results of the experimental data analysis. Although different signal to MDA ratios where calculated for the two datasets, these discrepancies do not appear to affect the requirements and conclusions between these cases. Therefore the GATE simulation study is considered to be validated on the particular cases where very low activity levels are involved and LSO intrinsic background is present.

As a result the conclusions from both experimental and simulated series of acquisitions can be used as a tool for designing and validating new acquisition clinical protocols, such as determining optimal levels of injected activity and acquisition lengths for the detection of small lesions, in the case where the operation of an LSO-based system at a point very close to its MDA parameter value is required.

ACKNOWLEDGEMENTS

The authors would like to thank the OpenGATE collaboration for allowing us to use the GATE simulation software for the purposes of this study. This work was also supported in part by UCLA SAIRP NIH-NCI 2U24 CA092865.

REFERENCES

[1] L.A. Currie, "Limits for Qualitative Detection and Quantitative Determination". *Application to Radiochemistry. Analytical Chemistry* 40(3):586-593; 1968.

[2] A. L. Goertzen, J. Y. Suk, C. J. Thompson, "Imaging of Weak-Source Distributions in LSO-Based Small-Animal PET Scanners", *Journal of Nuclear Medicine*.2007; 48: 1692-1698

[3] L. Eriksson, C. C. Watson, K. Wienhard, M. Eriksson, M. E. Casey, C.Knoess, M. Lenox, Z. Burbar, M. Conti, B. Bendriem, W. D. Heiss, and R. Nutt, "The ECAT HRRT: An example of NEMA scatter estimation issues for LSO-based PET systems," *IEEE Transactions on Nuclear Science*, vol. 52, pp. 90-94, 2005.

[4] C. C. Watson, M. E. Casey, L. Eriksson, T. Mulnix, D. Adams, and B. Bendriem, "NEMA NU 2 performance tests for scanners with intrinsic radioactivity," *Journal of Nuclear Medicine*, vol. 45, pp. 822-6, 2004.

[5] S. Yamamoto, H. Horii, M. Hurutani, K. Matsumoto, and M. Senda, "Investigation of single, random, and true counts from natural radioactivity in LSO-based clinical PET," *Ann Nucl Med,* vol. 19, pp. 109-14, 2005.

[6] S. Jan et al. "GATE: a simulation toolkit for PET and SPECT", Phys. Med. Biol. 49 (2004) 4543-4561

[7] Y C Tai, A. Chatziioannou, S. Siegel, J. Young, D. Newport, R.N. Goble, R.E. Nutt, S.R. Cherry, "Performance evaluation of the microPET P4: a PET system dedicated to animal imaging", *2001 Phys. Med. Biol.* 46 1845-1862

[8] D.B. Stout, A.F. Chatziioannou, T.P. Lawson, R.W. Silverman, S.S. Gambhir, M.E. Phelps "Small Animal Imaging Center Design: The Facility at the UCLA Crump Institute for Molecular Imaging" - Molecular Imaging and Biology, 2005 – Springer New York, Volume 7, Number 6 / November, 2005.

[9] K. Thielemans, D. Sauge, C. Labbe, C. Morel, M. Jacobsen and A. Zverovich, "STIR Softwrae for Tomographic Image Reconstruction: User's Guide, Version 1.3 Hammersmith Imanet, 2004", htttp://stir/irsl.org/documentation/STIR-UsersGuide.pdf